BNL-NUREG--45274

CONF-9010 2 DE91 004012

EFFECT OF BALANCE OF PLANT AND CONTROL SYSTEM FEEDBACK ON AMPLITUDE OF POWER AND FLOW OSCILLATIONS

W. Wulff, H. S. Cheng and A. N. Mallen
Brookhaven National Laboratory (BNL)
Upton, NY 11973, United States of America

ABSTRACT

The BNL Engineering Plant Analyzer (EPA) for BWR power plants predicts an amplitude of 1,300% of full power for limit-cycle, core-wide power oscillations after postulated scram failure at the LaSalle-2 power plant. This is larger than the TRAC-G predictions by General Electric (GE) and the RETRAN predictions by the Electric Power Research Institute. Modeling and computing errors in the EPA are analyzed here as potential causes for EPA's over-predictions of peak fission power. It is concluded that the EPA is more likely to under-predict than to over-predict fission power peaks. It is found that the omission of dynamic BOP feedback effects from TRAC-G modeling and the premature termination of TRAC-G calculations account for most of TRAC-G's under-prediction of the fission power peaks.

This work was sponsored under the auspices of the U. S. Nuclear Regulatory Commission.

1. INTRODUCTION

Computer simulations of the 1988 LaSalle BWR instability, carried out for the condition of postulated scram failure, at General Electric (GE) and at Brookhaven National Laboratory (BNL) produced limit-cycle power oscillations with widely differing amplitudes. GE results, as presented to the NRC in November 1989, showed maximum power oscillation amplitudes of 200% of normal full power, while BNL results showed at least seven times larger amplitudes. This discrepancy had to be resolved, since large power amplitudes lead potentially to fuel damage, and since for increasing fission power amplitude the time-averaged fission power also increases. This is shown by the top curve in Figure 1 below, which was obtained by simulating the LaSalle event with Scram failure on the Engineering Plant Analyzer (EPA) at BNL. In turn, the rise in time-averaged fission power can lead to an accelerated temperature rise in the pressure suppression pool, possibly requiring modifications in ATWS emergency procedures.

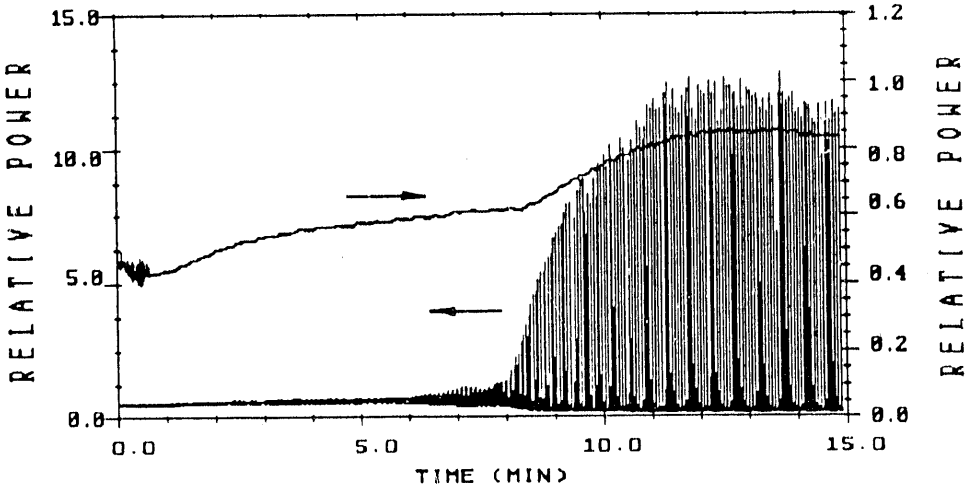

Figure 1. Fission Power Oscillations (with ordinate on the left) and Time-Averaged Power (top curve, with ordinate on the right) for LaSalle with Postulated Scram Failure.

The purpose of this paper is to resolve the difference between these power amplitude predictions, by presenting first the methods used at BNL for identifying, and then to identify, the potential causes of the discrepancy between GE and BNL predictions. Although applied specifically to the LaSalle instability, the methods used at BNL for sorting out potential computer code-related errors and uncertainties are useful in general to support computer predictions.

Separate analyses were performed for assessing the effects from (i) computing errors, (ii) modeling errors and (iii) errors made in imposing boundary conditions. Potential computing and modeling errors were assessed separately for neutron kinetics, thermal conduction in fuel and for thermohydraulics. All error analyses were carried out for the purpose of explaining why

the power amplitudes as predicted by the EPA at BNL exceeded those predicted by the TRAC-G computer code at GE.

We present below first the assessment of potential errors from computing and modeling. Then we demonstrate that the GE predictions of peak power are too low for two reasons, namely because

a. the resonance feedback from the Balance of Plant via feedwater injection was not modeled by GE, and
b. GE calculations were prematurely terminated at four minutes after onset of oscillations, while it takes about seven minutes to reach limit-cycle oscillations (see Figure 1 above).

2. EFFECTS FROM COMPUTATIONAL ERRORS ON PEAK POWER

Computational errors are the truncation errors arising from time and possibly from space discretizations of the governing equations. Computational errors were given first priority attention because of the exceptionally strong high-frequency content of the fission power oscillations. Most truncation errors cause under-predictions of amplitudes. However, through the interaction of void and Doppler reactivity feedback, some truncation errors could lead to over-predictions.

2.1 Neutron kinetics computations

Neutron kinetics computations are associated with uncertainties which arise from integrating the point kinetics equations and from predicting void and Doppler reactivity. The latter two are addressed in Sections 2.2 and 2 3 below.

The Engineering Plant Analyzer (EPA) utilizes the variable implicit integration method for prompt neutron kinetics equations, as reported earlier [1, pp. 3-16]. Nonoscillatory transients were simulated in the past on the EPA by this method and with the integration step size of 30.5 milliseconds. This step size was found to be too large for oscillatory transients, causing an under-prediction of fission power by 19.5 $\pm$ 2.1%, when the total reactivity exceeded temporarily one dollar during large-amplitude power oscillations. Based on the analysis described below, the time step was subsequently reduced to 4.36 milliseconds in the EPA which, in turn, reduced the power peak error to -1.4 $\pm$ 1.7% of the amplitude.

To quantify the above amplitude under-predictions from the point kinetics model in the EPA, two steps were taken by H. S. Cheng [2]: (i) a closed-form integration for each time step was used as a bench mark calculation and (ii) the EPA model was implemented in the advanced, high-precision simulation computer AD100 and executed with decreasing time steps until the time step was found which produced convergence and agreement with the benchmark calculation.

For the benchmark calculation, it was assumed that the fractions β_i of delayed neutrons, their decay constants λ_i and the prompt neutron generation time Λ are constant during an integration step. After normalizing and integrating the point kinetics equations, one obtains

$$n(\tau) = n(\tau_k) + \frac{1}{\Lambda}\int_{\tau_k}^{\tau} \rho(\tau')\cdot n(\tau')d\tau' - \frac{1}{\Lambda}\sum_i \frac{\beta_i}{\lambda_i}\left[c_i(\tau) - c_i(\tau_k)\right] \quad , \qquad (1)$$

where n and c_i denote the neutron density and precursor concentrations, respectively, both normalized by their respective initial values and ρ is the total reactivity. Integration of the precursor equations yields

$$c_i(\tau) = c_i(\tau_k)e^{-\lambda_i(\tau-\tau_k)} + \lambda_i\int_{\tau_k}^{\tau} e^{\lambda_i(\tau'-\tau)}n(\tau')d\tau' \quad . \qquad (2)$$

To facilitate the integrations in Eqs.(1) and (2), the normalized neutron density was approximated by

$$n(\tau) = \left[p_o + p_1(\tau - \tau_k)\right]e^{\omega(\tau-\tau_k)} \quad , \qquad (3)$$

where the constants p_o, p_1 and ω were derived, respectively, to satisfy initial and end conditions for n at $\tau = \tau_k$ and $\tau_k + \Delta\tau$, and to satisfy the differential equation for n. This provides these three equations for the unknown constants:

$$p_o = n(\tau_k), \quad p_1 = \frac{1}{\Delta\tau}\left[n(\tau_k + \Delta\tau)e^{-\omega\Delta\tau} - n(\tau_k)\right] \qquad (4)$$

$$p_1 - \left[e^{-\omega\Delta\tau}/\Lambda\right]\sum_i \beta_i c_i + (p_o + p_1\Delta\tau)\left[\omega - \frac{\rho - \beta}{\Lambda}\right] = 0 \qquad (5)$$

Equation (5) is transcendental in ω and solved by Newton Raphson iteration. The second of Eq.(4) contains the unknown neutron density at the end time $\tau_k + \Delta\tau$ of the time step. A predictor of ω and of the neutron density $n(\tau_k + \Delta\tau)$ are computed, respectively, from Eqs.(5) and (1), using p_1 from the previous time step, then p_1 is compared with the predictions. Then a corrector for $n(\tau_k + \Delta\tau)$ is obtained with the new p_1, and the process is repeated for the next time step.

The total reactivity is taken directly from the EPA as shown in Figure 2 below. Figure 3 shows the comparison of results from the benchmark calculations (solid line) and from the variable implicit method used in the EPA, with the integration step size of 4.357 milliseconds, as now adopted for all stability analyses with the EPA.

The mean of -1.4% and the standard deviation of 1.7% of the EPA under-prediction in power peaks were obtained from tabulated output data and are negligibly small when compared with the total uncertainty of predicting power peaks, which is still dominated by the uncertainties associated with reactivity predictions.

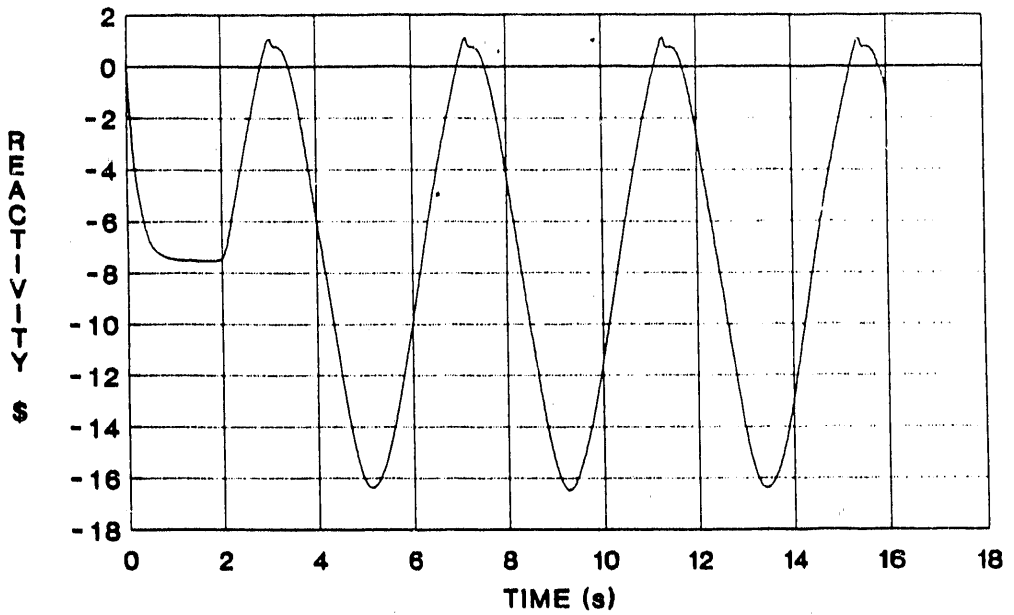

Figure 2. Total Reactivity, as obtained from EPA for LaSalle with postulated scram failure (for times of 2 seconds and greater) and used for benchmark calculations.

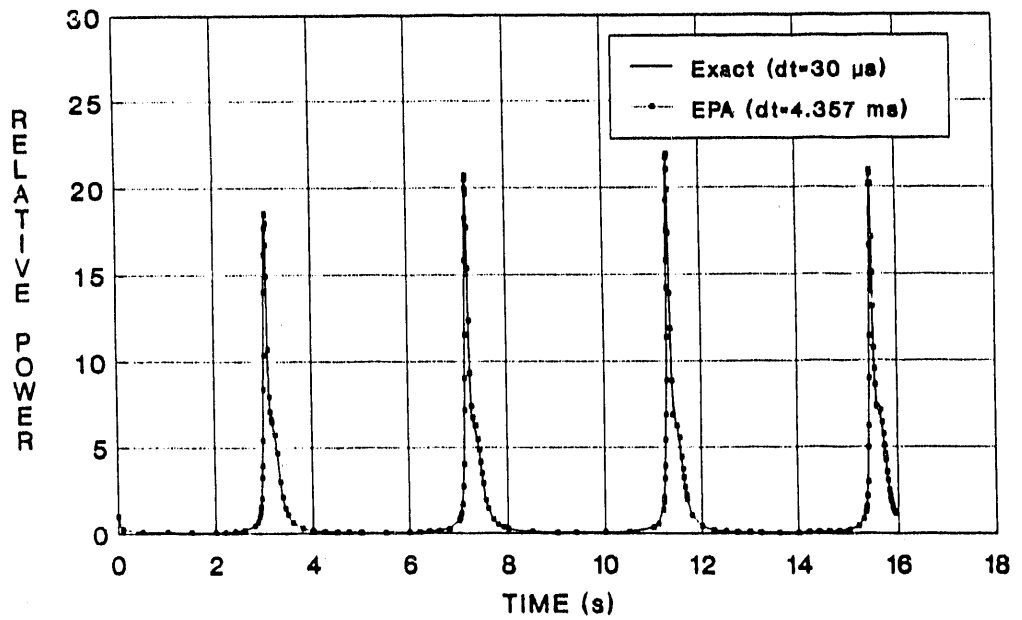

Figure 3. Comparison of Benchmark and EPA calculations, the latter with reduced integration time step.

2.2 Fuel temperature calculations

The fuel temperature calculations affect strongly the total reactivity via the contribution from Doppler reactivity. Figure 4 is a magnification of a section around the first peak in Figure 2. Shown are the component reactivities from void, Doppler and moderator temperature, along

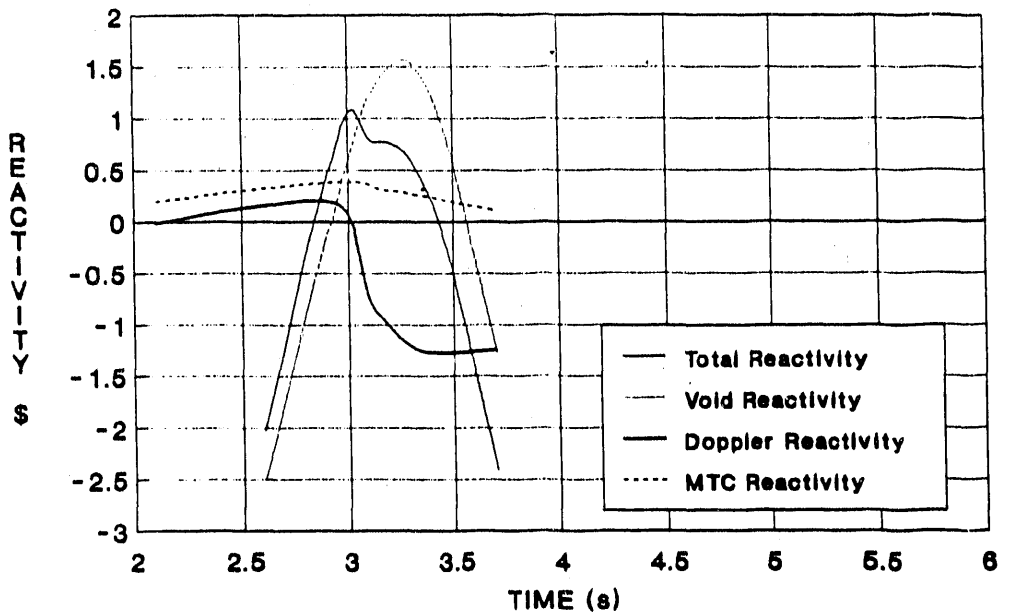

Figure 4. Components of reactivity at the time of maximum reactivity.

with the total reactivity. Figure 4 shows how the total reactivity reaches its peak, even while the void reactivity is still rising, primarily because of the sharp drop in Doppler reactivity, which occurs just when the total reactivity peaks. Thus, Figure 4 demonstrates the important contribution of fuel temperature to the prediction of power peaks.

The fuel temperature is computed in the EPA by a lumped-parameter model [1, pp. 3-23 through 3-35], which is derived by integral techniques. This model requires the integration of ordinary differential equations only, requiring the assessment of only time-discretization errors. The errors arising from the modeling approximations of radial temperature distributions are discussed below in Section 3.2.

Integration time step variations, imposed on the algorithm for fuel temperatures predictions, showed that convergence is achieved within less than 2% of fuel temperature amplitude for time step sizes less than five milliseconds. For practical reasons of multi-stepping strategies in the EPA, the same integration time step of 4.357 milliseconds is being used for predicting fuel temperatures, fission power and Doppler reactivity.

The reduction of the integration step size from 30.5 to 4.357 milliseconds reduced the peak power from 2,900 to 2,200% of normal full power, but it increased the time-averaged power by 25%, from 90 to 115% of rated power, due to the broadening of the power spikes.

2.3 Thermohydraulics calculations

Numerical Diffusion. Thermohydraulics calculations in the EPA give rise to only insignificant errors from the quadratures in space for the mixture mass and momentum balances [1, pp. 3-45 through 3-54], but also to the more important errors of numerical diffusion from

integrating the partial differential equations for vapor mass and mixture energy conservation [1, pp. 3-54 through 3-56].

The integration of these two balance equations is achieved by explicit first-order (Euler) time, and donor-cell space differencing. This method has numerical diffusion which is quantified through its numerical diffusivity [2, p. 148].

$$\nu_n = (v/2)\,(\Delta z - v\Delta t) \quad , \tag{6}$$

where v denotes the fluid velocity, while Δz and Δt denote space and time increments, respectively. Numerical diffusion reduces to zero, as the Courant number $N_{co} = v\Delta t/\Delta z$ approaches unity from below. The explicit method is unstable for $N_{co} \geq 1$, but it is for any given choice of Δt and Δz more accurate than implicit integration [2, p. 155].

In order to minimize numerical diffusion of the hydraulics calculations in the EPA, the time step for integrating the vapor mass and mixture energy equations is selected to achieve the largest possible Courant number just below unity.

Time and space discretization studies with 8, 12 and 24 axial subdivisions were performed with the RAMONA-3B computer code which now has the same thermohydraulics models and integration algorithms as the EPA. These truncation error analyses were performed for steady-state and small power oscillations, keeping the Courant number fixed. Convergence within 2% has been obtained for predicting steady-state void distributions and the maximum gain in the power-to-flow transfer function, by using the twelve axial subdivisions in the EPA.

For large power oscillations, the Courant number was first decreased in the EPA and then the trend observed for increasing Courant numbers, but fixed axial nodalization. It is estimated from this study that the EPA underpredicts the power peaks by approximately 20% and the mean power by approximately 2% due to numerical diffusion. A more definite estimation of the numerical diffusion requires finer axial subdivisions and therefore the use of the advanced AD100 computer in the EPA, because the AD10 lacks the necessary memory capacity.

Numerical diffusion must be ruled out for explaining the difference between TRAC-G calculations at GE and EPA simulations at BNL; on account of numerical diffusion in the EPA, the difference can be only larger than observed.

Numerical Exitation. Based on simplified computational examples, ORNL staff has suggested that the large limit-cycle oscillations predicted by the EPA could be exited by the explicit, first-order Euler integration method, because the imaginary axis is excluded from the numerical stability domain of that method, and because the reactor system may have poles on that axis. This suggestion, however, was indisputably refuted by utilizing the unique simulation features of the EPA: all first-order Euler integration methods were interactively, through short key board commands, replaced by first, second and fourth-order Adams-Moulton, Adams-Bashford and Runge-Kutta integration methods, for all of which the numerical stability domain includes segments of the imaginary axis. The same oscillations were obtained as before, with

the average peak of 1,273% and the standard deviation of 52% of full power, while the original first-order Euler method produced the peak of 1,230%.

It must be concluded that the oscillations predicted by the EPA originate in its mathematical models and not in its numerical methods. Moreover, none of the computational uncertainties discussed in Section 2 above could possibly lead to an over-prediction of fission power peaks.

3. EFFECTS FROM MODELING ERRORS ON PEAK POWER

Modeling errors arise from the use of specific models, such as point, instead of 3D, kinetics or lumped parameter, instead of finite difference, conduction models, and from the uncertainties in the constitutive relations.

3.1 Neutron kinetics

Neutron kinetics in the point kinetics model of the EPA are affected primarily by uncertainties in reactivity feedback models. The void coefficients are taken from GE data for LaSalle-2 [3, Fig. 6-2, p. 34 (proprietary)]. Doppler coefficients and moderator temperature coefficients were taken from [4] and [5], respectively, and confirmed by GE data.

The initial axial power distribution was taken from actual LaSalle power plant data and matched by the EPA within 3% of actual local values. Transient axial power shape variations are simulated in the EPA by approximating, at each one of twelve axial locations, actual transient LaSalle power shape data taken during the first seven minutes before scram. The approximation was achieved through a first-order Taylor series expansion in terms of local void fraction, local fuel temperature and local moderator temperature [2, App. B]. The agreement achieved by the EPA can be seen in Figure 5. The maximum error is 3%.

The radial power distribution effects are approximated in the EPA by the use of one spatial weight factor each for void, Doppler and moderator temperature [4]. These weight factors are, respectively, 1.35, 1.052 and 1.00 for steady state conditions and 1.43, 1.25 and 1.00 for transient conditions. The respective reactivity coefficients are multiplied by these weight factors. In addition, a hot channel factor is applied to the fission power for the hot channel fuel temperature calculation. The simulation of radial power distribution gives undoubtedly rise to the greatest uncertainty in neutron kinetics, however this uncertainty is small when compared to the difference between GE and BNL calculations. EPA-predicted time for onset of oscillations, for the occurrence of scram, and the predicted growth rate of oscillations agree well with LaSalle plant data [2, Ch. 2]. This tends to confirm the above kinetics parameters.

3.2 Fuel temperature

Fuel temperature predictions affect Doppler reactivity and wall heat flux calculations. The lumped-parameter fuel conduction model of the EPA was compared with analytical and finite difference models under conditions of periodically varying fission power, for the purpose

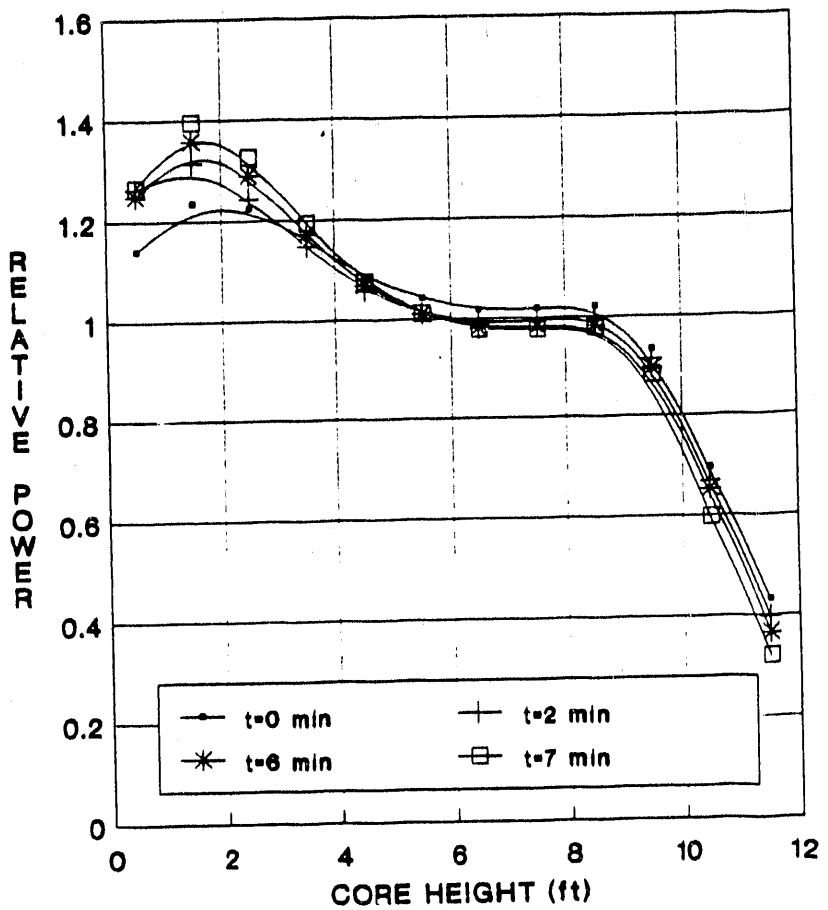

Figure 5. Comparison of Transient Axial Power Distribution from the LaSalle Plant (symbols) and the Engineering Plant Analyzer (lines).

of assessing the error in the amplitudes of the volume-averaged pellet temperature and of the wall heat flux at the outer cladding surface [2, App. D].

The analytical solution was derived for the cylindrical pellet with peripheral heat transfer resistance equal to the series of resistances from gap, cladding and coolant boundary layer. The fission power was taken to vary sinusoidally with time. The oscillatory part for the analytical solution is, in normalized form

$$<\tilde{\Theta}_f> \;=\; 4\sum_{n=1}^{\infty} \frac{\sin\left[\omega\tau \;-\; arctg\left(\omega/\lambda_n^2\right)\right]}{\lambda_n^4\left[1+\left(\lambda_n^2/N_{Bi}\right)\right]\;\sqrt{1\;+\;(\omega/\lambda_n)^2}} \qquad \textit{(analytical model)} \qquad \textbf{(7a)}$$

where $\tau = \alpha_f t / R_f^2$ is the normalized time, $\omega = 2\pi f R_f^2/\alpha_f$ the normalized frequency, $\Theta_f = (T_f - T_{sat})kf/(R_f^2 \cdot q_o''')$ the normalized temperature, $N_{Bi} = h_c R_f / k_f$ the Biot number, R_f, k_f and α_f are, respectively the pellet radius, thermal conductivity and thermal diffusivity, t is time and f is the frequency of power oscillations, q_o''' is the amplitude of fission power density oscillation, while λ_n denotes the eigenvalues obtained from $\lambda_n \cdot J_1(\lambda_n) = N_{Bi} \cdot J_o(\lambda_n)$.

Using the same integral methods as in the EPA, the lumped-parameter model corresponding to the above analytical model yields for the oscillatory part

$$<\tilde{\theta}_f> = \frac{\sin[\omega\tau - arctg(\omega/\lambda^2)]}{\sqrt{\lambda^4 + \omega^2}} , \qquad (lumped - parameter\ model) \qquad (7b)$$

where $\lambda^2 = 8N_{Bi}/(4 + N_{Bi})$ which equals λ_1 in Eq.(7a) for small values of λ_1. By evaluating Eqs.(7) for the actual frequencies obtained by the EPA, it is shown that the amplitude error for fuel temperature and Doppler reactivity feedback is 1.8% and that the peaks have a 24 millisecond phase shift. It should be noted that the asymptotic time mean of the lumped-parameter model has no error relative to the analytical solution.

The wall heat flux affects void generation in the moderator. The analytical solution gives for the oscillatory part of normalized wall heat flux

$$(\tilde{q}_w'')^* = \frac{\tilde{q}_w''}{R_f q_o'''} = \sum_{n=1}^{\infty} \frac{2\sin[\omega\tau - arctg(\omega/\lambda^2)]}{\sqrt{\lambda_n^4 + \omega^4\left[1 + (\lambda_n^2/N_{Bi})^2\right]}} , \qquad (analytical\ model) \qquad (8a)$$

while the corresponding result from the lumped parameter solution is

$$(\tilde{q}_w'')^* = \frac{\sin[\omega\tau - arctg(\omega/\lambda^2)]}{2\sqrt{1 + (\omega/\lambda^2)^2}} , \qquad (lumped - parameter\ model) . \qquad (8b)$$

By evaluating Eqs.(8) for the frequency of LaSalle's large-amplitude oscillations, one finds that the EPA under-predicts the amplitude by only 3% of the mean heat flux, but by 35% of the relatively small amplitude itself, and that there is a phase lag of 46 miliseconds in the 4.2 second period. Since this relatively large underprediciton of wall heat flux amplitude is expected to cause an underprediciton of fission power amplitude, it was decided to determine first the nonlinear effects from the actual fission power (see Fig. 3, showing the nonsinusoidal fission power variation) on wall heat flux amplitude, and then the effects on peak fission power, from the actual under-prediction of heat flux.

A standard finite difference model for thermal conduction in fuel pellet and cladding [6, p. 270], was implemented on the AD100 simulation computer, with varying numbers of radial subdivisions. The results show that for large-amplitude power oscillations:

(i) 10 and 4 radial subdivisions are needed in pellet and cladding, respectively, to achieve 3-digit convergence in the wall heat flux predictions,

(ii) with only 4 and 2 subdivisions, there is a 7% error, with 3 and 1 subdivisions, the error is 12% for wall heat flux predictions,

(iii) the EPA over-predicts the minimum wall heat flux by 28% and under-predicts the maximum wall heat flux by 24%.

The 28% over-prediction of minimum wall heat flux affects the power peaks directly because the minimum heat flux dictates the minimum void fraction and maximum positive reactivity.

Because of program memory limitations in the AD10 system of the EPA, the detailed finite difference model used in the above analysis could not by utilized in the EPA. In order to quantify the closed-loop feedback effect of the heat flux amplitude under-prediction in the EPA, the computed wall heat flux q''_w was fed as input signal x to a digital second-order lead-lag compensator, the output y of which was used for all subsequent calculations of vapor generation and as input to the mixture energy equation. The lead-lag compensator is represented by

$$y(t) = x(t) - p(t), \quad \dot{p} = -C_1 p + C_2(x - p - r), \quad \dot{r} = C_3(x - p - r)$$

$$p(o) = O, \quad r(o) = x(o) \quad ,$$

where the constants C_1, C_2 and C_3 are computed such that the transfer function $P(s) = Y(s)/X(s)$ provides with $P(o) = 1$ that the mean heat flux remains unaltered, with $|P(i\omega)| = m$ the required amplitude magnification m, and finally with $tg\varphi = I\{P(i\omega)\}/R\{P(i\omega)\}$ the required phase shift φ.

Figure 6 shows the result of the cladding wall heat flux correction for the under-prediction by the lumped-parameter model in the EPA. The fission power peak increased, as a result of this error compensation, from 1,283% to 1,360% of normal full power, or by 6%.

A more rigorous error assessment requires the implementation of the detailed conduction model in the entire BWR simulation code for the AD100. But the under-prediction of the peak fission power is not expected to exceed 12%.

3.3 Thermohydraulics modeling

Thermohydraulics modeling uncertainties are caused primarily from the uncertainties of those modeling parameters which affect thermohydraulic stability. The EPA employs best-estimate correlation for form losses at core entrance and exit (GE design data, NEDE-31428P, 1988), fuel gap conductance (GE design data), boiling wall heat transfer (Jens-Lottes), drift flux (GE design data for rod bundles), two-phase multipliers (EPRI NP-1924-CCM, 1981) and wall shear (Martinelli-Nelson-Jones).

A separate analysis was performed to demonstrate that the location of net vapor generation incipience is always near the core entrance because of the strong bottom power peaking and low core flows which prevailed at LaSalle. Therefore, there is no strong effect on peak power expected from uncertainties in predicting this location.

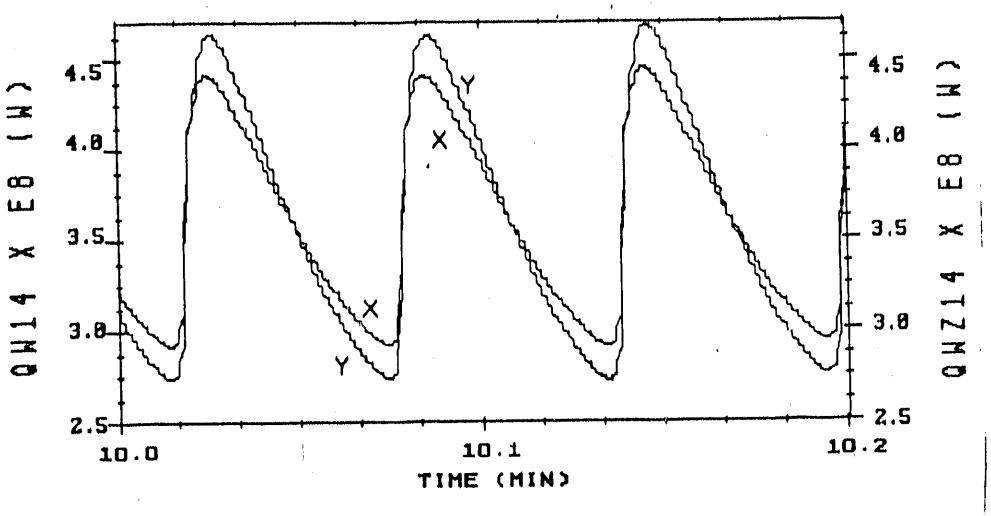

Figure 6. Wall Heat Flux Amplification to compensate for amplitude under-prediction in EPA. X is input, Y is output signal, the amplification is 28%.

While the uncertainties from thermohydraulics modeling in the EPA were shown, by comparison with test and plant data, to be small for moderate power oscillations, there is no data base for comparisons under conditions of large-amplitude power oscillations, particularly when dryout and rewetting occur in the core. Although this observation has no bearing on the resolution of the issues concerning the discrepancies in peak power predictions, the uncertainties in simulating post-critical heat flux conditions in oscillating flows have an enormous impact on assessing fuel damage.

4. EFFECTS FROM BOUNDARY CONDITIONS

The EPA simulates Balance of Plant (BOP) components with standard dynamic models for pumps and turbines, valves, valve actuators and for heat exchangers [1, Sects. 3.7-3.14]. The EPA simulates also the control and plant protection systems dynamically [1, Sects. 3.15 and 3.16] with plant-specific control parameters and trip set points.

A fundamental difference between TRAC-G calculations and EPA simulations of the LaSalle instability with postulated scram failure arises from the difference in imposition of boundary conditions. GE calculations [7] were performed by imposing, from the time the fission power exceeded the scram set point, constant feedwater flow and temperature, these two being kept fixed at the values they reached at that time, as is shown by curves (c) and (d) in Figure 7 below. In contrast, the LaSalle instability with postulated scram failure has been simulated before by the EPA without the imposition of feedwater boundary conditions, since these had been simulated dynamically: feedwater mass flow rate had been simulated so as to maintain coolant inventory in the vessel (see curve (a) in Figure 7), while feedwater temperature had been

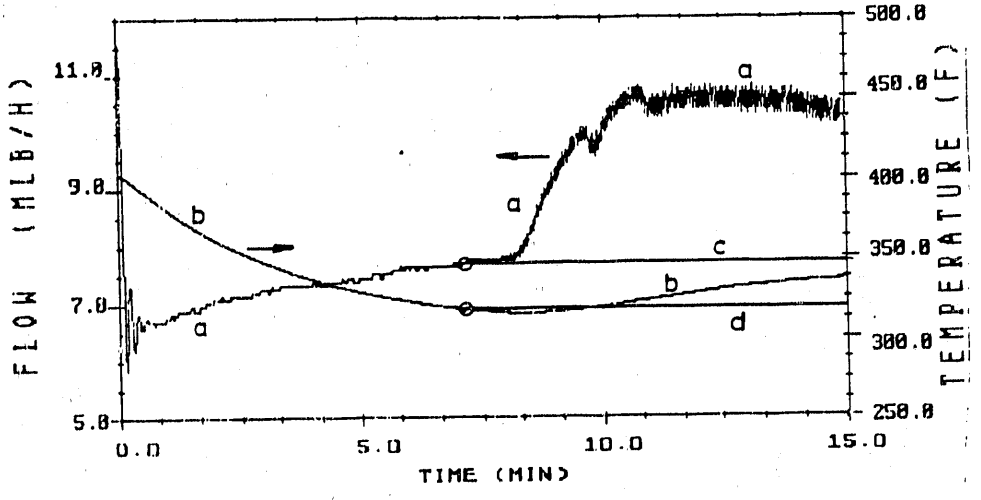

Figure 7. Feedwater Mass Flow Rate (a) and Temperature (b) as simulated dynamically in the EPA, curves (c) and (d) as imposed for TRAC-G calculations.

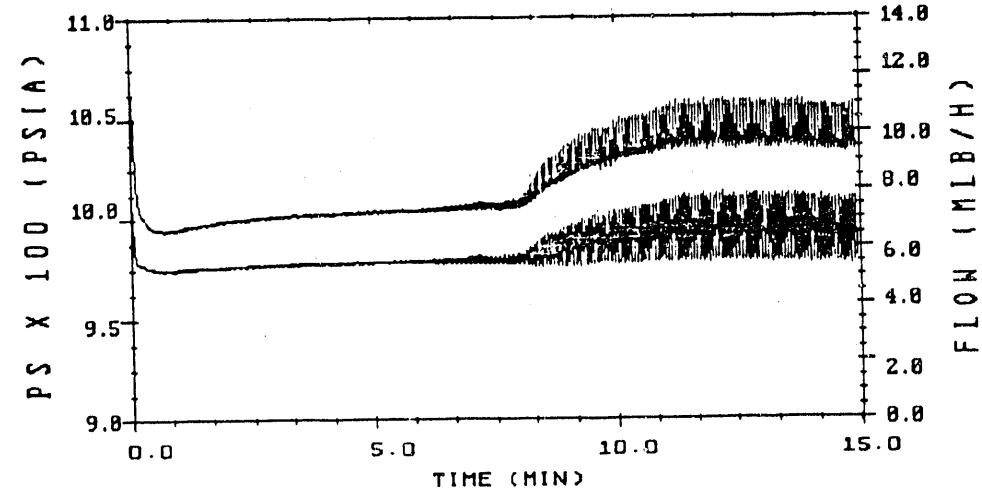

Figure 8. Pressure and Steam Flow Oscillations, obtained from the EPA during large limit-cycle power oscillations.

simulated dynamically from the heat transfer between extraction steam and feedwater (curve (b) in Figure 7). Figure 8 shows the EPA-simulated vessel pressure and mass flow in the steam line. The associated fission power was shown before in Figure 1 above.

Notice that according to the dynamic EPA simulation the feedwater flow continues to rise after scram conditions are exceeded, and to oscillate at the same frequency as the fission power. Similarly, the dome pressure and steam flow also rise and oscillate. Both the change in mean values and the oscillations must be expected to have a feedback effect on the amplitude of limit-

cycle power oscillations, even though they have obviously no effect on the decay ratio at the onset of instabilities.

The effect of imposing fixed feedwater flow and temperature as boundary conditions has been assessed by repeating the EPA simulation with feedwater conditions as shown by curves (c) and (d) in Figure 7, keeping everything else the same as for Figure 1. This imposition of fixed boundary conditions reduced both the amplitude and the rise of the mean fission power oscillations by the factor of 3.5, thereby demonstrating the importance of feedback effects from the Balance of Plant (BOP). As stated in the introduction, the incorrect simulation of BOP feedback effects in TRAC-G is a major reason in under-predicting the fission power amplitude for limit-cycle oscillations.

5. GROWTH TIME FOR LIMIT-CYCLE OSCILLATIONS

Figure 1 shows, that, starting from the time at which oscillations occur, it takes about seven minutes for the limit-cycle power oscillation to reach maximum amplitudes. TRAC-G calculations were prematurely terminated after four minutes. After four minutes, EPA reaches only 80% of the maximum amplitude.

Superposition of TRAC-G on EPA results for the early time of amplitude growth shows in Figure 9 that the EPA predicts lower amplitudes than TRAC-G. This suggests that the EPA is more likely to under-predict than to over-predict the fission power amplitude.

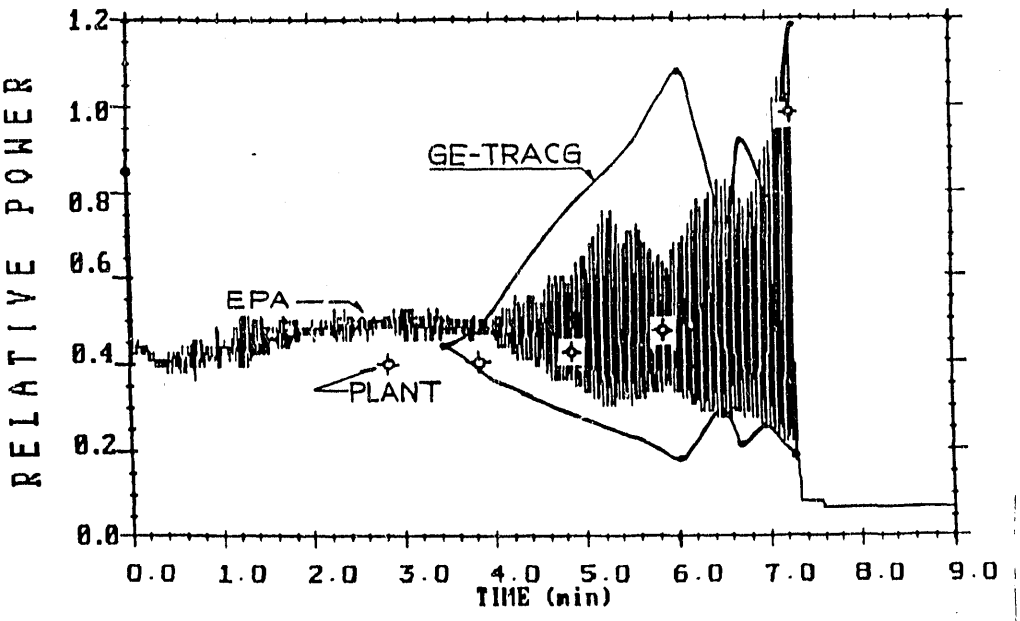

Figure 9. Superposition of TRAC-G and EPA Predictions of Fission Power Amplitude Growth, during first four minutes after onset of oscillations.

6. CONCLUSIONS

No computing or modeling errors in the EPA could be identified as causes responsible for the discrepancy by a factor of seven or more between TRAC-G and EPA predictions for the amplitude of limit-cycle power oscillations.

The omission in TRAC-G of dynamically simulating the BOP feedback effects, and the premature termination of the TRAC-G calculations account for a difference by the factor of 4.7 in the predicted amplitude of limit-cycle power oscillations. The major contribution to the discrepancy between TRAC-G and EPA predictions arises from the omission of BOP feedback effects in TRAC-G.

REFERENCES

[1] Wulff, W., H. S. Cheng, S. V. Lekach and A. N. Mallen: "The BWR Plant Analyzer", Plant Analyzer Development Group, Department of Nuclear Energy, Brookhaven National Laboratory, Upton, Long Island, New York 11973, NUREG/CR-3943, 1984.

[2] Cheng, H. S., A. N. Mallen, U. S. Rohatgi and W. Wulff: "BWR Instability Analysis With the BNL Engineering Plant Analyzer", Plant Analyzer Development Group, Department of Nuclear Energy, Brookhaven National Laboratory, Upton, Long Island, New York 11973, 1990.

[3] Pearson, H. J.: "LaSalle Unit 2 Reload-2 Nuclear Design Report", NEDE-31428P, Proprietary Report, General Electric Company, 1988.

[4] Cheng, H. S. and D. J. Diamond: "BWR Doppler Feedback Effects of Voids, Control Blades, Gadolina and Exposure", Brookhaven National Laboratory, BNL-NUREG-24433, 1978.

[5] Cheng, H. S. and D. J. Diamond: "Reactivity Transients During a Blowdown in MSIV Closure ATWI", Trans. American Nuclear Society (1988) Vol. 57, 147-148.

[6] Lahey, R. T. Jr. and F. J. Moody: The Thermal Hydraulics of a Boiling Water Reactor, American Nuclear Society (1977).

[7] Shang, J. C.: "Plant Stability Qualification", BWROG, presented before the ACRS Thermal Hydraulics Phenomena Subcommittee, BWR Topical Meeting, San Francisco, CA, November 8 & 9, 1989.

END

DATE FILMED

12/12/90